Chapter 6

REMOVAL OF CHROMIUM USING NANO CRYSTALLINE IRON OXIDE/HYDROXIDE

In this chapter the capability of adsorption of chromium on synthesized nano crystalline iron oxide/hydroxide is discussed. Additionally, effect of various parameters and their significance on removal (%) of chromium is assessed. The isotherm and kinetic parameter determination by linear and nonlinear methods are reported. Thermodynamic parameters are also determined for explaining feasibility and nature of the adsorption process involved in the system.

6.1. Adsorption Experiments

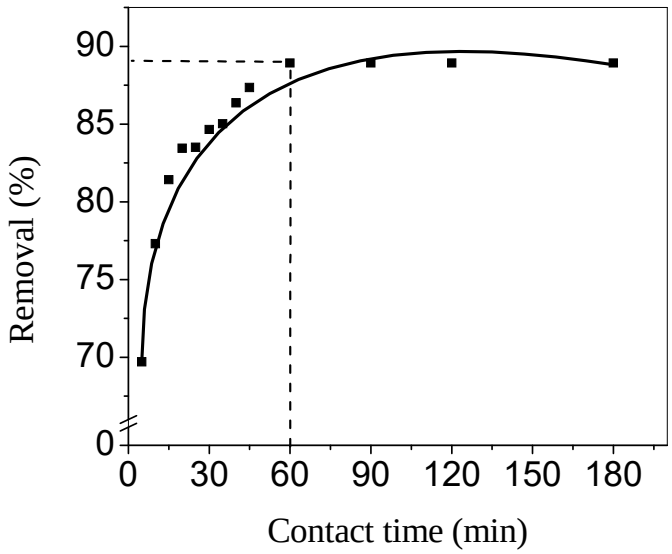

Figure 6.1 Effect of contact time on removal (%) of chromium from aqueous solution on nano crystalline iron oxide/hydroxide (initial concentration = 10 mg L^{-1}, pH = 6.6, adsorbent dose = 2 g L^{-1}, agitation speed= 120 rpm temperature =303K)

The equilibrium contact time for adsorption of chromium by nano crystalline iron oxide/hydroxide was found out to be 60 min (Figure 6.1). The preliminary experiments for adsorption of chromium on nano crystalline iron oxide/hydroxide were studied by variation of pH from 2 to 10 (Figure 6.2 A). The chromium removal (%) decreased with increase of pH. The maximum removal was achieved at pH 2. In effect of adsorbent dose study (Figure 6.2 B), the chromium removal (%) becomes stagnant after adsorbent dose of 6 g L^{-1}. In study of effect of initial concentration; the chromium removal (%) decreased with increase of initial concentration. In addition to this, the chromium removal (%) declines with rise of temperature (Figure 6.2). On the basis of preliminary studies, the experimental conditions in RSM are taken as pH in range of 2 to 10, adsorbent dose in range of

4 to 8 g L^{-1}, initial concentration in the range of 20 of 50 mg L^{-1} and temperature in the range of 303 to 313 K.

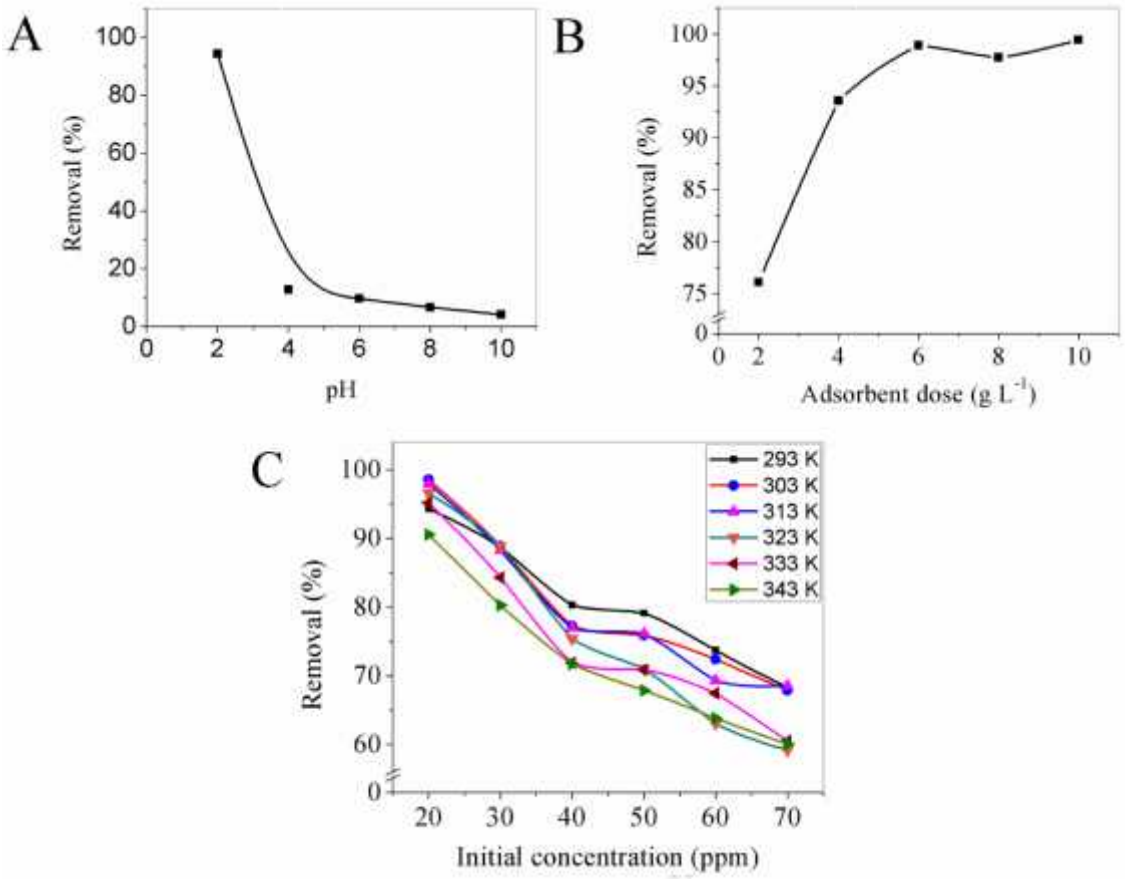

Figure 6.2 (A) Effect of pH (adsorbent dose = 4 g L^{-1}, initial concentration = 20 mg L^{-1}, temperature = 303 K) (B) Effect of adsorbent dose (Initial pH=2, initial concentration = 20 mg L^{-1}, temperature = 303 K) (C) Effect of initial concentration on removal of chromium using nano iron oxide/hydroxide (adsorbent dose = 4 g L^{-1}, initial pH =2)

6.1.1. Data analysis and construction of regression

Regression equation for removal of chromium by adsorption on nano crystalline iron oxide/hydroxide is generated by regression analysis of the data:

$$Y = 12.73 - 3.01\,(\text{initial concentration}) - 43.52\,(\text{pH}) + 3.17\,(\text{adsorbent dose}) - 0.8484\,(\text{temperature}) + 1.98\,(\text{initial concentration})^2 + 36.51\,(\text{pH})^2 - 1.93\,(\text{adsorbent dose})^2 - 1.12\,(\text{temperature})^2 + 2.12\,(\text{initial concentration x pH}) + 1.2816\,(\text{initial concentration x adsorbent dose}) - 0.1678\,(\text{initial concentration x temperature}) - 2.42\,(\text{pH x adsorbent dose}) + 0.5368\,(\text{pH x temperature}) + 0.2464\,(\text{adsorbent dose x temperature}) \quad (6.1)$$

Here Y represents the removal (%) of chromium.

Table 6.1 Experimental runs for removal of chromium utilizing nano crystalline iron oxide/hydroxide

Run Order	Initial conc.	pH	Adsorbent Dose	Temp.	Removal (%)		Run Order	Initial conc.	pH	Adsorbent Dose	Temp.	Removal (%)
	(mg L^{-1})		(g L^{-1})	(K)				(mg L^{-1})		(g L^{-1})	(K)	
1	20	2	4	303	95.39		16	50	8	8	313	3.87
2	20	8	4	303	5.08		17	35	2	6	308	93.62
3	20	2	8	303	99.92		18	35	8	6	308	3.20
4	20	8	8	303	8.13		19	35	5	4	308	9.87
5	50	2	4	303	80.01		20	35	5	8	308	10.05
6	50	8	4	303	3.185		21	20	5	6	308	16.45
7	50	2	8	303	96.98		22	50	5	6	308	11.30
8	50	8	8	303	5.127		23	35	5	6	303	10.77
9	20	2	4	313	92.62		24	35	5	6	313	10.77
10	20	8	4	313	3.185		25	35	5	6	308	12.10
11	20	2	8	313	99.18		26	35	5	6	308	8.985
12	20	8	8	313	7.26		27	35	5	6	308	15.23
13	50	2	4	313	74.39		28	35	5	6	308	12.10
14	50	8	4	313	3.875		29	35	5	6	308	15.23
15	50	2	8	313	94.19		30	35	5	6	308	15.23
							31	35	5	6	308	15.23

The empirical model in terms of actual parameters (uncoded) is written in general form as follows:

$$Y = - 3967.12 - 0.6214 \text{ (initial concentration)} - 65.32 \text{ (pH)} + 0.3172 \text{ (adsorbent dose)} + 27.36 \text{ (temperature)} + 0.0088 \text{ (initial concentration)}^2 + 4.05 \text{ (pH)}^2 - 0.4828 \text{ (adsorbent dose)}^2 - 0.0451(\text{temperature})^2 + 0.0471223 \text{ (initial concentration x pH)} + 0.0427208 \text{ (adsorbent dose x initial concentration)} - 0.00223675 \text{ (initial concentration x temperature)} - 0.404131 \text{ (pH x adsorbent dose)} + 0.0357847 \text{ (pH x temperature)} + 0.0246378 \text{ (adsorbent dose x temperature)} \quad (6.2)$$

The regression equation (Equations 6.1 and 6.2) include the non significant terms to maintain hierarchical nature of the model (Zheng *et al.* 2011). The coefficient of determination with 80% or more value predicts good fit of the regression model (Yuliwati *et al.* 2012). Chromium removal with iron oxide/hydroxide have regression coefficient more than 99% (Table 6.2). Hence, regression model explained the adsorption of chromium on nano iron oxide/hydroxide in current range of conditions (Sarkar and Majumdar 2011). R^2_{pred} and R^2_{adj} were 98.28 and 99.40 (Table 6.2). It showed very high chances of model to predict the response at any new set of conditions within the experimental conditions.

Table 6.2 Estimated regression coefficients for removal of chromium by nano crystalline iron oxide/hydroxide

Term	**Coef**	**SE Coef**	**p**
Constant	12.7319	0.8818	0
Initial concentration	-3.0166	0.7006	0.001
pH	-43.5209	0.7006	0
Adsorbent dose	3.1723	0.7006	0
Temperature	-0.8484	0.7006	0.244
Initial concentration * Initial concentration	1.9843	1.8452	0.298
pH*pH	36.5156	1.8452	0
Adsorbent dose *Adsorbent dose	-1.9314	1.8452	0.311
Temperature*Temperature	-1.1276	1.8452	0.55
Initial concentration*pH	2.1205	0.7431	0.011
Initial concentration* Adsorbent dose	1.2816	0.7431	0.104
Initial concentration*Temperature	-0.1678	0.7431	0.824
pH* Adsorbent dose	-2.4248	0.7431	0.005
pH*Temperature	0.5368	0.7431	0.481
Adsorbent dose *Temperature	0.2464	0.7431	0.745
S = 2.9726 , PRESS = 762.90			
R-Sq = 99.68, R-Sq(pred) = 98.28%, R-Sq(adj)= 99.40%			

Magnitude of coefficient indicates towards strength of particular variable (Table 6.2). The sign afore to the variable gives the information about its positive or negative effect on chromium removal (%). The increase in parameter with positive sign afore to its coefficient led to increase of chromium removal (%) *or vice versa* (Sarkar and Majumdar 2011). pH was most dominating factor as suggested by highest magnitude of coefficient and sum of squares. This is followed by

adsorbent dose, initial concentration and temperature. Negative sign afore to coefficient of pH suggests the decrease in removal (%) of chromium with rise of pH. So, maximum chromium removal (%) was achieved with lowest feasible pH for adsorption process. Negative sign was also afore to the coefficient of initial concentration suggests the decrease in the chromium removal (%) with rise of initial concentration. Negative sign is also afore to the coefficient of temperature, but it is non-significant. The p value of more than 0.05 was the reason for non significant effect of temperature. Adsorbent dose was next dominating factor after pH. It has positive sign afore to its coefficient, it suggested the increase in the removal of chromium with increase in adsorbent dose. Square term of pH only was significant with p value less than 0.05 (Table 6.2). Interaction of 'pH-adsorbent dose' and 'pH- initial concentration' was significant ($p < 0.5$).

Table 6.3 Analysis of Variance for removal of chromium utilizing nano crystalline iron oxide/hydroxide

Source	DF	Seq SS	Adj SS	Adj MS	F	p
Regression	14	44303.2	44303.2	3164.5	358.12	0
Linear	4	34451.1	34451.1	8612.8	974.7	0
Initial concentration	1	163.8	163.8	163.8	18.54	0.001
pH	1	34093.2	34093.2	34093.2	3858.29	0
Adsorbent dose	1	181.1	181.1	181.1	20.5	0
Temperature	1	13	13	13	1.47	0.244
Square	4	9653.8	9653.8	2413.4	273.13	0
Initial concentration*Initial concentration	1	7.7	10.2	10.2	1.16	0.298
pH*pH	1	9634.2	3460.4	3460.4	391.6	0
Adsorbent dose * Adsorbent dose	1	8.5	9.7	9.7	1.1	0.311
Temperature*Temperature	1	3.3	3.3	3.3	0.37	0.55
Interaction	6	198.3	198.3	33.1	3.74	0.016
Initial concentration*pH	1	71.9	71.9	71.9	8.14	0.011
Initial concentration* Adsorbent dose	1	26.3	26.3	26.3	2.97	0.104
Initial concentration*Temperature	1	0.5	0.5	0.5	0.05	0.824
pH* Adsorbent dose	1	94.1	94.1	94.1	10.65	0.005
pH*Temperature	1	4.6	4.6	4.6	0.52	0.481
Adsorbent dose*Temperature	1	1	1	1	0.11	0.745
Residual Error	16	141.4	141.4	8.8		
Lack-of-Fit	10	105.2	105.2	10.5	1.74	0.257
Pure Error	6	36.2	36.2	6		
Total	30	44444.6				

6.1.2. ANOVA

ANOVA was applied to the data for model fitness and significance of the effects (Table 6.3).The p value less than 0.05 suggest the term to be significant. The pH, initial concentration and adsorbent dose were significant terms among linear effects. Square term of pH and interaction term of 'pH-adsorbent dose' and 'pH-initial concentration' was significant. The adjusted sum of squares also suggested pH was most dominating factor followed by adsorbent dose, initial concentration and temperature.

6.1.3. Effect of initial concentration

Initial concentration is third major dominating factor after pH and adsorbent dose with penultimate least sum of squares (Table 6.3). The chromium removal (%) decreased with increase in the initial concentration of the adsorbate (Figure 6.3). The unsaturated sites on the adsorbent are limited. At low initial concentration, relatively high numbers of sites were available for adsorption for same adsorbent dose. So, the removal (%) of chromium was high. On increasing initial concentration, saturation of active sites was increased, which led to less number of active sites available for the adsorption. Hence, adsorbate concentration in the solution increased which led to decrease in removal (%) of chromium with increase in concentration.

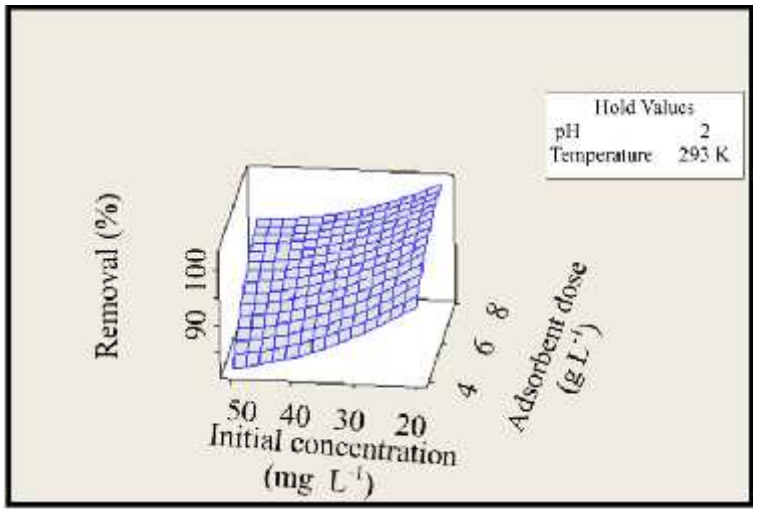

Figure 6.3 Surface plot of 'chromium removal (%) *vs.* adsorbent dose (g L^{-1}) and initial concentration (mg L^{-1})' at hold values of pH and temperature at 2 and 293 K respectively

Surface Plot (Figure 6.4) of 'chromium removal (%) *vs.* pH and initial concentration' depicts a marginal decrease in chromium removal (%) at constant pH. This depicts larger effect of pH on chromium removal (%) as compared to initial concentration.

6.1.4. Effect of pH

The pH has the highest sum of squares (Table 6.3) for removal of chromium using nano iron oxide/hydroxide, so it was the most dominating factor. The removal (%) of chromium declines with rise of pH of the solution (Figures 6.4 and 6.5).

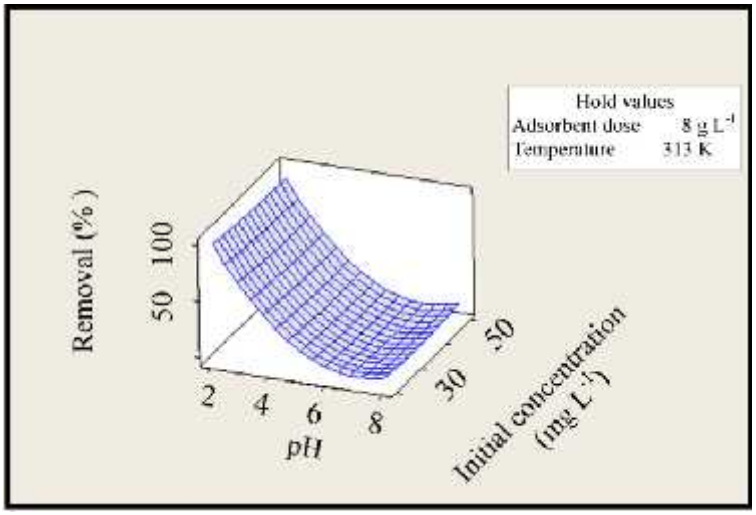

Figure 6.4 Surface plot of 'chromium removal (%) *vs.* pH and initial concentration (mg L^{-1})' at hold values of adsorbent dose and temperature at 8 g L^{-1} and 313 K respectively

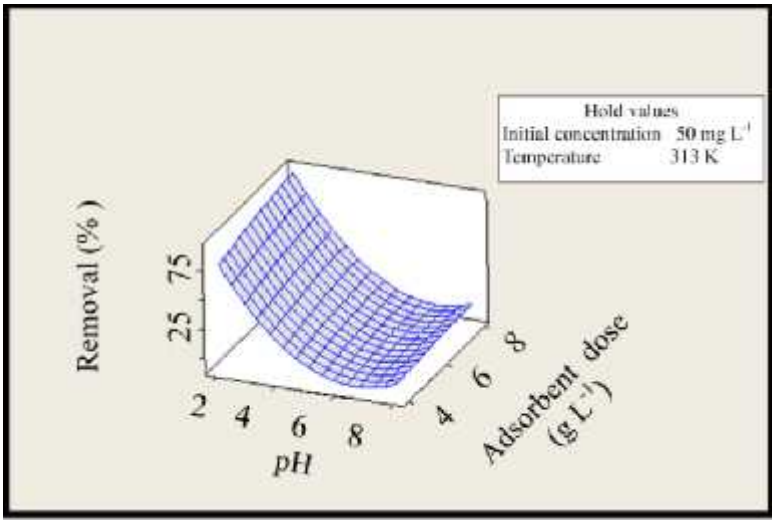

Figure 6.5 Surface plot of 'chromium removal (%) *vs.* pH and adsorbent dose (g L^{-1})' at hold values of initial concentration and temperature at 50 mg L^{-1} and 313 K respectively

The chromium exists in three oxidation states in the aqueous solution i.e. $HCrO^{4-}$,$Cr_2O_7^{2-}$and $Cr_4O_{13}^{2-}$ (Kiran and Kaushik 2008). The decline in pH of the solution leads to increase of positive surface charge on adsorbent. So, the electrostatic force of attraction increased between the adsorbent and adsorbate with increase of positive charge on the surface of adsorbent. The difference in chromium removal (%) at extreme pH in the study was vast (Experimental run '1,2'; '3,4'; '5,6'; '7,8' in Table 6.1). A very high amount of chromium removal (%) is achieved at lower pH. The $HCrO^{4-}$ form of chromium increased in solution with decrease in pH (Bajpai *et al.* 2012). Hence, the adsorption affinity was high for $HCrO^{4-}$ as compared to the other forms of chromium. This can be credited to high e/m (charge/mass) ratio of $HCrO^{4-}$. The pH_{zpc} of the adsorbent is 7.65, hence electrostatic force was dominating below this pH and adsorption above this pH is governed by other mechanism apart from electrostatic nature.

6.1.5. Effect of adsorbent dose

Adsorbent dose was the most dominating factor after pH for removal of chromium using iron oxide/hydroxide. In this case the sum of squares was next highest to pH (Table 6.3). The rise and declination of removal (%) of chromium followed opposite trend as in case of effect of initial concentration. The chromium removal (%) increased with increase of adsorbent dose or *vice versa*. The increase of number of active sites for adsorption sites was higher with adsorbent dose and it was reason for higher removal (%). Response surface plot (Figure 6.3) depicted maximum removal in extreme ends of adsorbent dose (4 and 8 g L^{-1}) at lower initial concentration (20 mg L^{-1}). The slope in response surface plot at higher initial concentration (50 mg L^{-1}) was higher as compared to lower initial concentration (20 mg L^{-1}). This suggested difference in the number of active sites at higher and lower initial concentration with variable adsorbent doses.

6.1.6. Effect of temperature

Temperature did not affect adsorption of chromium significantly.

6.1.7. Response surface and contour plots

Response surface and contour plots for chromium removal using iron oxide/hydroxide are represented in Figure 6.3 to 6.8. Response surface and contour plots (Figure 6.4 to 6.6) depicted that higher chromium removal (%) was achieved in lower pH range. The Figure 6.5 depicts that the effect of adsorbent dose have minimal effect on removal (%) of chromium at hold value of 50 mg L^{-1} initial concentration. The contour plots are parallel lines (Figures 6.6 and 6.7) indicated absence of any interaction between parameters. In contour plot (Figure 6.8); the contour lines are twisted. The twisted lines signify the interaction between the terms i.e. adsorbent dose and initial concentration (Figure 6.8) at lower pH (Myers *et al.* 2009).

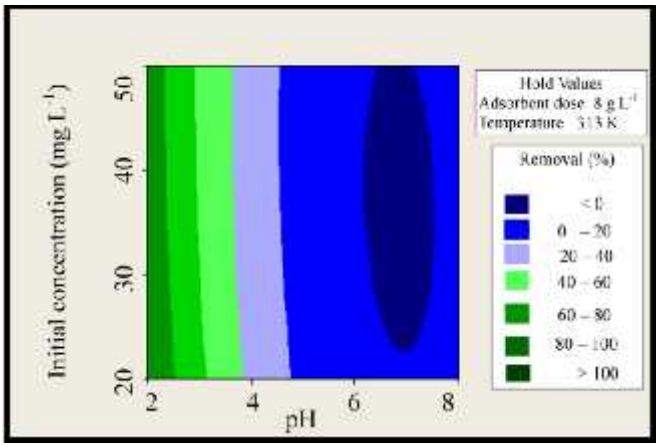

Figure 6.6 Contour plot of 'chromium removal (%) *vs.* pH and initial concentration (mg L^{-1})' at hold values of adsorbent dose and temperature at 8 g L^{-1} and 313 K respectively

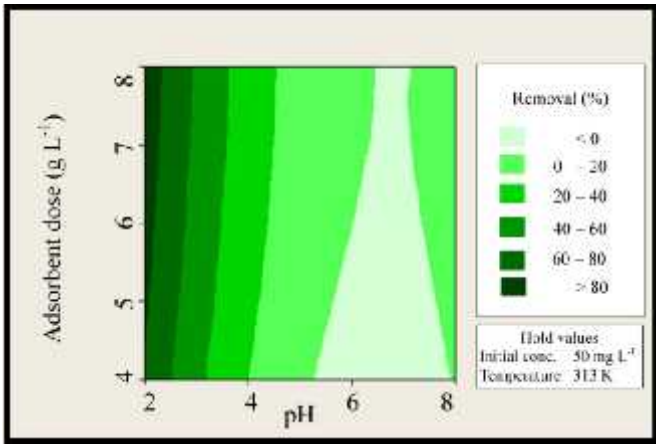

Figure 6.7 Contour plot of 'chromium removal (%) *vs.* pH and adsorbent dose (g L^{-1})'at hold values of initial concentration and temperature at 50 mg L^{-1} and 313 K respectively

The Figure 6.7 also depicts that adsorbent dose also does not depicted any effect on removal (%) in acidic pH (at or below pH 4 with hold value of 50 mg L^{-1} initial concentration). The high chromium removal (%) is predicted with decreased initial concentration and increased adsorbent dose (Figures 6.3 and 6.8). So, response surface and contour plots depicted higher removal (%) at acidic pH, high adsorbent dose and low initial concentration.

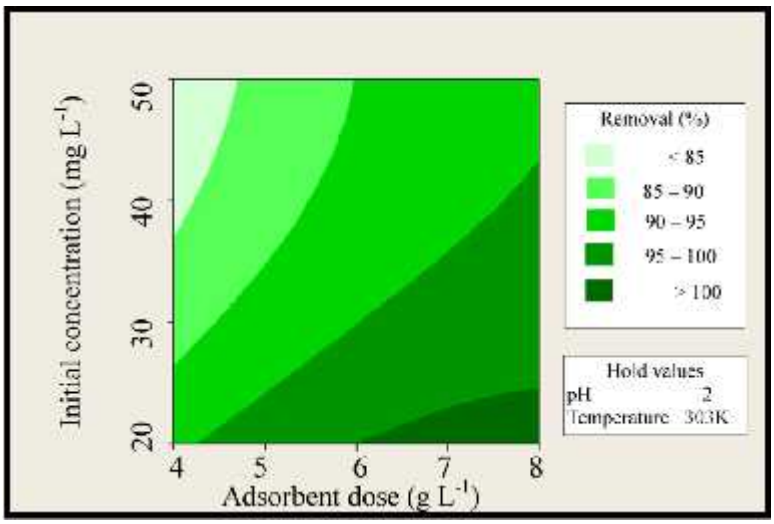

Figure 6.8 Contour plot of 'chromium removal (%) *vs.* adsorbent dose (g L^{-1}) and initial concentration (mg L^{-1})' at hold values of pH and temperature at 2 and 293 K respectively

6.1.8. Confirmation experiments

Optimization of removal of chromium is achieved by optimization plot (Figure 6.9) on the basis of experimental results generated by Minitab 16 software. The optimum conditions for chromium removal by nano iron oxide/hydroxide were as follows: initial pH = 2, initial chromium concentration = 21.83 mg L^{-1}, adsorbent dose = 7.99 g L^{-1}, Temperature= 303 K (Figure 6.9). Verification of the predicted results by the regression model was conducted at aforementioned conditions. The experimental results were in close proximity of the predicted results (Table 6.4). It validated the high efficiency of the model. However, confirmation experiments at higher pH were not close to the predicted response. It depicted the validity of the model at lower pH.

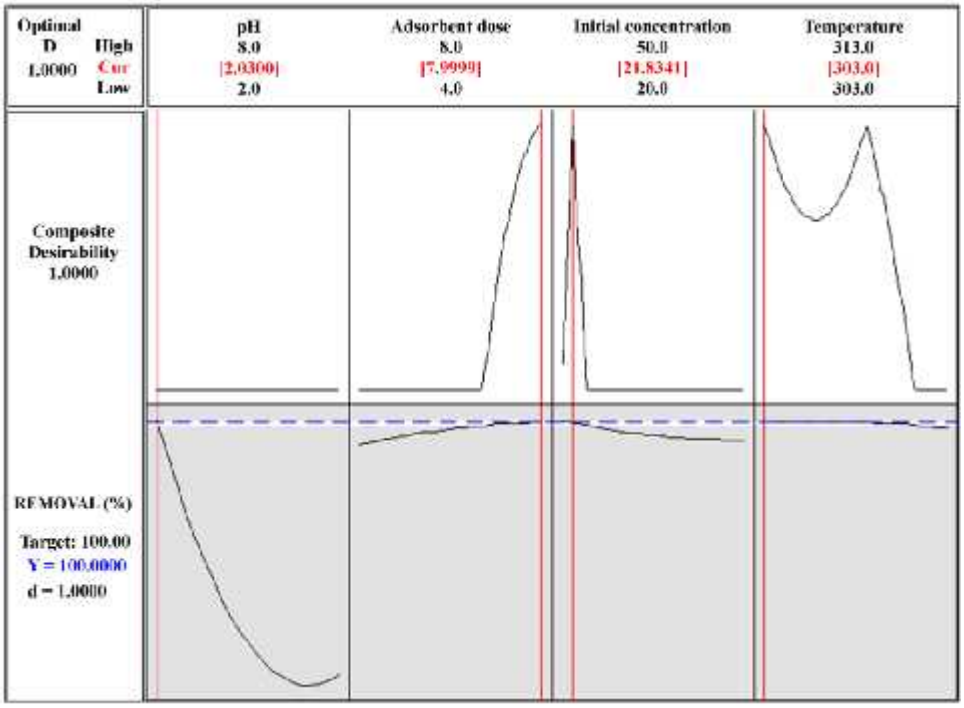

Figure 6.9 Optimisation plot of removal of chromium from aqueous solution by iron oxide/hydroxide

Table 6.4 Confirmation experiments for removal of chromium using nano crystalline iron oxide/hydroxide

S.No.	Initial conc. (mg L^{-1})	pH	Adsorbent dose (g L^{-1})	Temperature (K)	Experimental values	Predicted values
1	22	3	8	303	59.68	65.05
2	38	2	6	303	95.68	92.15
3	42	4	6	303	48.09	29.96
4	48	3	8	303	58.56	59.57
5	50	4	5	303	51.8	26.63
6	20	6	4	303	46.35	3.18
7	28	6	6	303	44.89	3.25
8	40	8	5	303	59.68	3.94

The complete removal of chromium was achieved by variation in pH and adsorbent dose (Table 6.5). The results suggested that the maximum removal of chromium was achieved at initial concentration = 20 mg L^{-1}, pH = 2-2.5 and adsorbent dose of 11 g L^{-1} and temperature = 303 K.

Table 6.5 Optimization of removal of chromium using nano iron oxide/hydroxide

S.No.	Initial conc. (mg L^{-1})	pH	Adsorbent dose (g L^{-1})	Temperature (K)	Removal (%)
1	20	2	8	303	99.37
2	20	2	9	303	99.65
3	20	2	10	303	99.69
4	20	2	11	303	100
5	20	4	12	303	100
6	20	2	11	303	100
7	20	2.5	11	303	100
8	20	3	11	303	46.7
9	20	3.5	11	303	40.8
10	20	4	11	303	41.85

6.2. Linear approach for isotherm analysis

The linear Langmuir isotherm plot (Figure 6.10) and Freundlich isotherm plot (Figure 6.11) depicts that the predicted data is proximate to experimental data. However, data predicted was much more proximate to experimental data in Langmuir isotherm plot than Freundlich isotherm plot (Figure 6.11) at few points.

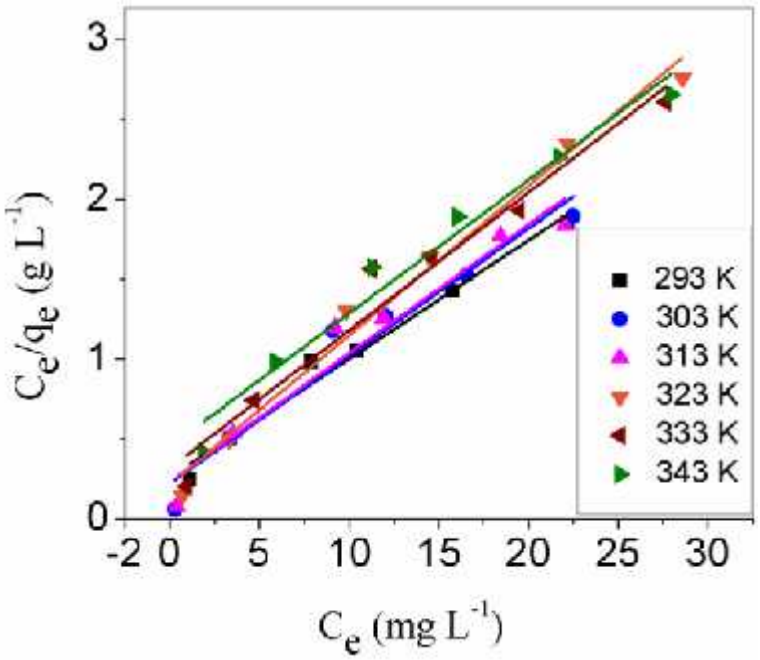

Figure 6.10 Linear Langmuir isotherm plot of chromium removal using nano crystalline iron oxide/hydroxide (dots represent the experimental data and lines represent the data estimated by the model)

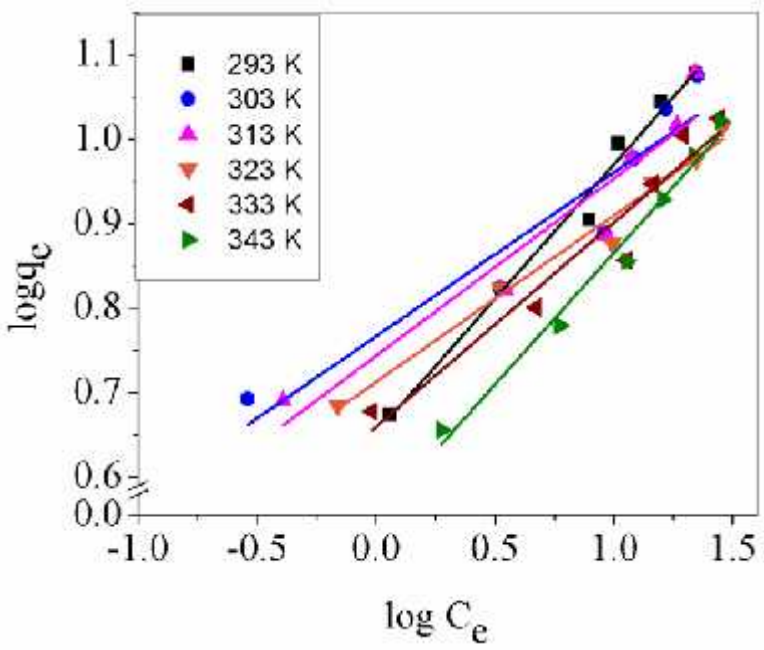

Figure 6.11 Linear Freundlich isotherm plot of chromium removal using nano crystalline iron oxide/hydroxide (dots represent the experimental data and lines represent the data estimated by the model).

Adsorption isotherm parameters determined with the help of linear analysis (Figures 6.10 and 6.11) are presented in Table 6.6.The slope and intercept of plots C_e/q_e versus C_e yields Langmuir constant values i.e. Q_o and b. The value of Q_o declines with temperature. The declination in the value of Q_o portrays decreased maximum adsorption capacity with rise of temperature. The values of K_F and 1/n were calculated from the intercept and slope of plot '$\log q_e$ *vs.* $\log C_e$'. Coefficient of determination was better for Langmuir isotherm as compared with Freundlich isotherm model (Table 6.6). So, linear isotherm analysis advocated the adsorption of chromium by iron oxide/hydroxide follows Langmuir isotherm model.

Table 6.6 Langmuir and Freundlich isotherm parameters along with coefficient of determination by linear analysis for adsorption of chromium from aqueous solution on nano crystalline iron oxide/hydroxide

		Langmuir parameters			Freundlich parameters		
Analysis method	**Temp. (K)**	**Q_o (mg/g)**	**b (L/mg)**	**R^2_{adj}**	**K_F ((mg/g) $(L/mg)^{1/n}$)**	**1/n**	**R^2_{adj}**
Linear	293	13.46	0.2866	0.9766	4.486	0.3184	0.9829
	303	12.51	0.3625	0.9396	5.845	0.1941	0.8754
	313	12.40	0.3471	0.9377	5.542	0.2101	0.8919
	323	10.68	0.4379	0.9827	5.162	0.1970	0.9773
	333	11.58	0.2720	0.9542	4.570	0.2415	0.9205
	343	11.97	0.1851	0.9645	3.574	0.3126	0.9785

6.3. Nonlinear approach for isotherm analysis

The nonlinear Freundlich isotherm plot (Figure 6.13) depicts the vast difference between the experimental data and data predicted by error analysis method. The data predicted by error analysis method depicted in Langmuir isotherm plot (Figure 6.12) is closer to experimental data than in Freundlich isotherm plot (Figure 6.13). However, the data predicted by error analysis method in Langmuir isotherm plot (Figure 6.12) is also less proximate to experimental data.

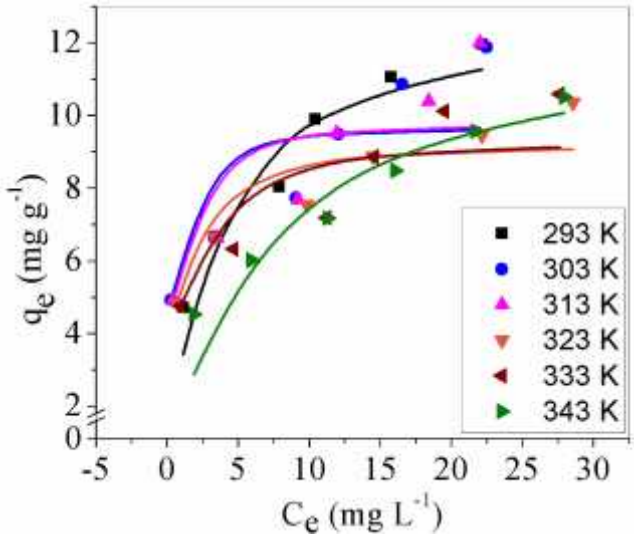

Figure 6.12 Nonlinear Langmuir isotherm plot of chromium removal using nano crystalline iron oxide/hydroxide obtained by error analysis method (dots represent the experimental data and lines represent the data estimated by the model)

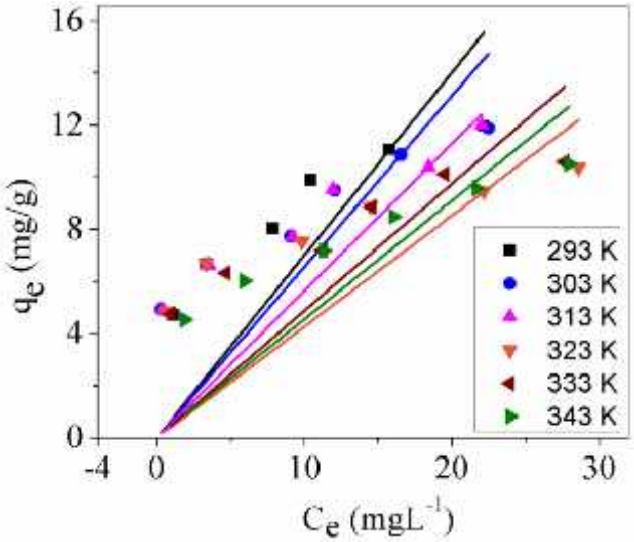

Figure 6.13 Nonlinear Freundlich isotherm plot of chromium removal using nano crystalline iron oxide/hydroxide obtained by error analysis method (dots represent the experimental data and lines represent the data estimated by the model)

The computed isotherm parameters with their coefficient of determination by customized Microcal origin (Figures 6.14 and 6.15) and error analysis methods (Figures 6.12 and 6.13) are presented in Tables 6.8 and 6.7 respectively. In error analysis method, the error function with lowest normalized sum of error function is selected as optimum error function for isotherm model. The parameter determined from the optimum isotherm model is selected for analysis. MPSD AND EABS explained four and two systems, respectively out of six systems better than other functions. Three systems in Freundlich isotherm analysis were better explained by EABS. ARE and ERRSQ explained one and two systems, respectively better than other error function. Coefficient of determination is used to determine the best suitable isotherm model. The higher value of coefficient of determination for Langmuir isotherm suggests better fit of data on Langmuir isotherm model. The negative values of coefficient of determination for Freundlich isotherm suggest the method cannot predict the Freundlich isotherm parameters (Table 6.7).

Table 6.7 Langmuir and Freundlich isotherm parameters along with coefficient of determination by error analysis method for adsorption of chromium from aqueous solution on nano crystalline iron oxide/hydroxide

	Langmuir parameters				**Freundlich parameters**			
Temp. (K)	**Error function**	**Q_o (mg/g)**	**b (L/mg)**	**R^2_{adj}**	**Error function**	**K_F {(mg/g (L/mg)$^{1/n}$)}**	**1/n**	**R^2_{adj}**
293	MPSD	12.86	0.3178	0.8415	EABS	0.8582	0.8169	-1.6055
303	MPSD	9.706	3.5692	0.2755	EABS	0.8052	0.8150	-1.7169
313	MPSD	9.847	2.4389	0.3221	ARE	0.5641	1	-1.8220
323	EABS	9.264	1.5842	0.6354	EABS	0.5955	0.7162	-4.6940
333	MPSD	9.436	1.0598	0.4819	ERRSQ	0.742	0.6568	-2.2716
343	EABS	12.29	0.1622	0.7551	ERRSQ	0.669	0.6798	-1.3410

Nonlinear analysis was performed using Microcal origin software. The nonlinear Langmuir isotherm plot (Figure 6.14) depicts the vast difference at three temperatures (293 K, 333 K and 343 K) between the experimental data and data predicted by customized Microcal origin function. The data predicted by customized Microcal origin function depicted in Freundlich isotherm plot (Figure 6.15) is closer to experimental data than in Langmuir isotherm plot (Figure 6.14).

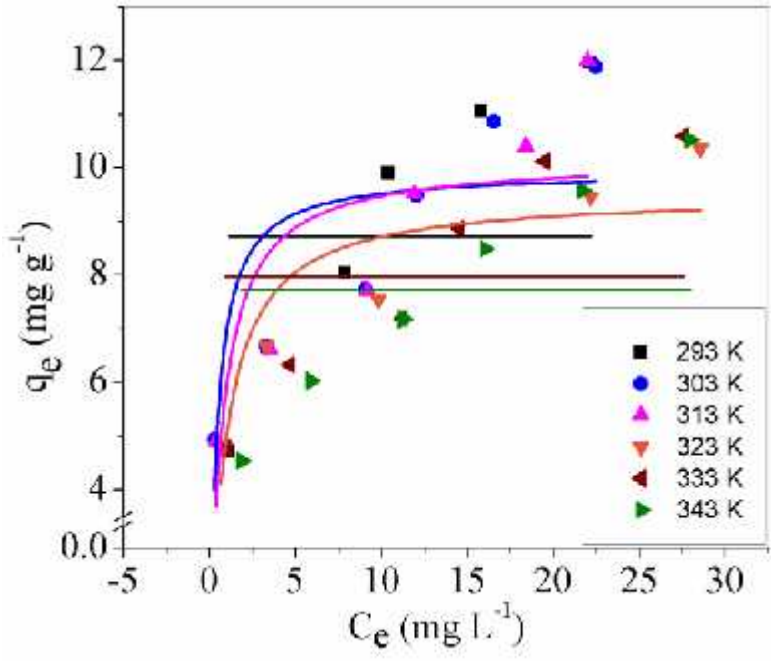

Figure 6.14 Nonlinear Langmuir isotherm plot of chromium removal using nano crystalline iron oxide/hydroxide obtained by customized Microcal origin function (dots represent the experimental data and lines represent the data estimated by the model)

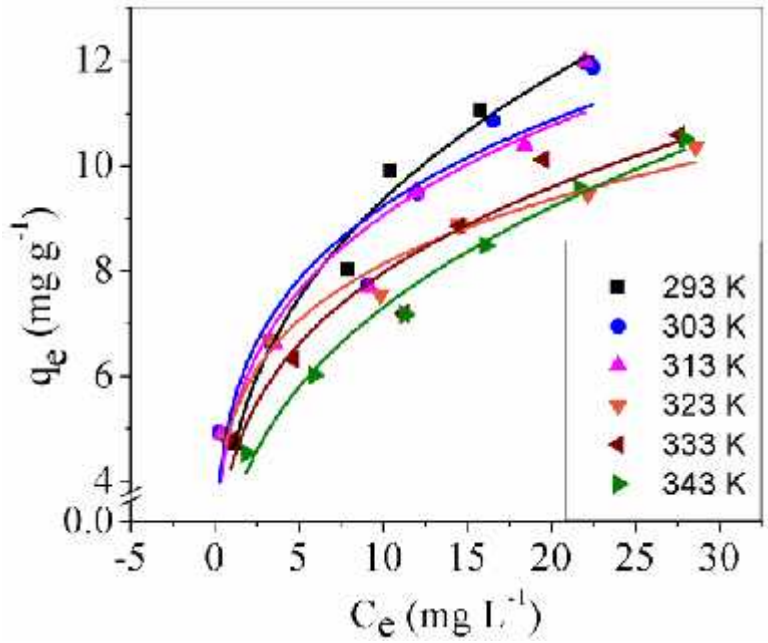

Figure 6.15 Nonlinear Freundlich isotherm plot of chromium removal using nano crystalline iron oxide/hydroxide obtained by customized Microcal origin function (dots represent the experimental data and lines represent the data estimated by the model)

Coefficient of determination also suggests that the data better fits on Freundlich isotherm (Table 6.8). Linear and nonlinear analysis using error function suggested that the Langmuir isotherm is a better model for the system. Microcal origin

suggests that the Freundlich isotherm to be a better model. On the basis of higher R^2_{adj}, isotherm parameters system follows Langmuir isotherm model and parameters calculated by linear analysis are preferred.

Table 6.8 Langmuir and Freundlich isotherm parameters along with coefficient of determination by Microcal origin for adsorption of chromium from aqueous solution on nano crystalline iron oxide/hydroxide

		Langmuir parameters			**Freundlich parameters**		
Analysis method	**Temp. (K)**	**Q_o (mg/g)**	**b (L/mg)**	**R^2_{adj}**	**K_F ((mg/g) $(L/mg)^{1/n}$)**	**1/n**	**R^2_{adj}**
Microcal origin	293	8.7183	$1.24 * 10^{45}$	-0.2500	4.448	0.3227	0.9786
	303	9.9201	2.3393	0.4789	5.359	0.2360	0.8742
	313	10.1439	1.4011	0.5283	5.091	0.2501	0.8838
	323	9.5007	1.1020	0.7593	5.086	0.2036	0.9716
	333	7.9726	$-5.71 * 10^{45}$	-0.2500	4.288	0.2687	0.9168
	343	7.7170	$1.52 * 10^{45}$	-0.2500	3.371	0.3357	0.9807

6.4. Linear analysis of Kinetic data

The linear pseudo-first order plot (Figure 6.16) showed the predicted data is proximate to most of the experimental data except at few data points (323 K and 343 K).

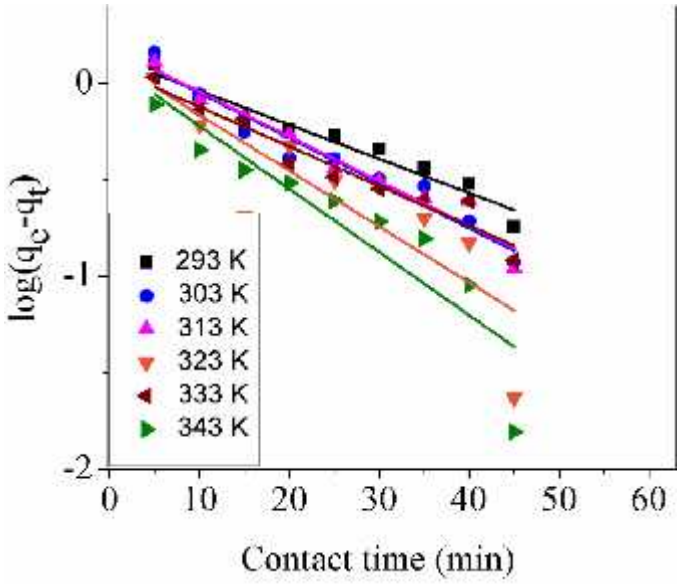

Figure 6.16 Linear pseudo-first order plot of chromium removal using nano crystalline iron oxide/hydroxide (dots represent the experimental data and lines represent the data estimated by the model)

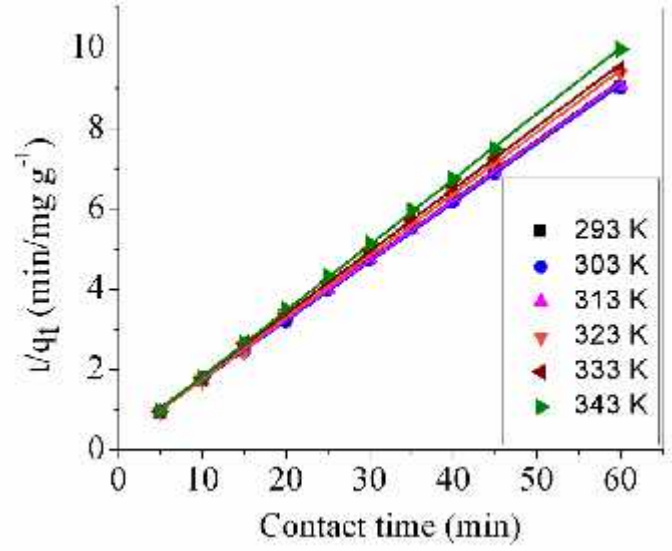

Figure 6.17 Linear pseudo-second order plot of chromium removal using nano crystalline iron oxide/hydroxide (dots represent the experimental data and lines represent the data estimated by the model)

The linear pseudo-second order plot also (Figure 6.17) depicts the close proximity of experimental and predicted data. However, the data predicted for pseudo-second order in the plot (Figure 6.17) depicts more proximity of experimental data to predicted data than depicted by pseudo-first order plot (Figure 6.16). The kinetic parameters determined by linear analysis (Figures 6.16 and 6.17) are presented in Table 6.9. On the basis of coefficient of determination and closeness of theoretical q_e to experimental q_e, pseudo-second order model fits the data better than pseudo-first order model. Hence, on the basis of linear model analysis, data is better fitted on pseudo-second order model.

Table 6.9 Pseudo-first order and pseudo-second order kinetic parameters by linear analysis for adsorption of chromium from aqueous solution on nano crystalline iron oxide/hydroxide

			Pseudo-first order			Pseudo-second order		
Analysis	**Temp. (K)**	**Experimental q_e (mg/g)**	**q_e (mg/g)**	**k_1 (min^{-1})**	**R^2_{adj}**	**q_e (mg/g)**	**k_2 (g $mg^{-1}min^{-1}$)**	**R^2_{adj}**
Linear	293	6.56	1.3735	0.0406	0.9430	6.7613	0.0726	0.9985
	303	6.66	1.5242	0.0537	0.9441	6.8152	0.0778	0.9995
	313	6.62	1.5393	0.0533	0.9521	6.7681	0.0764	0.9994
	323	6.39	1.3346	0.0666	0.6701	6.5104	0.1075	0.9991
	333	6.32	1.2093	0.0472	0.9312	6.4296	0.0918	0.9993
	343	6.02	1.2756	0.0753	0.8047	6.1218	0.1362	0.9997

6.5. Nonlinear approach for kinetic model analysis

The nonlinear pseudo-first plot (Figure 6.18) depicts a lesser amount of proximity between the experimental data and data predicted by error analysis method. The nonlinear pseudo-second order plot (Figure 6.19) depicts the close proximity between the experimental data and data predicted by error analysis method and the proximity was much more than depicted by pseudo-first plot (Figure 6.18).

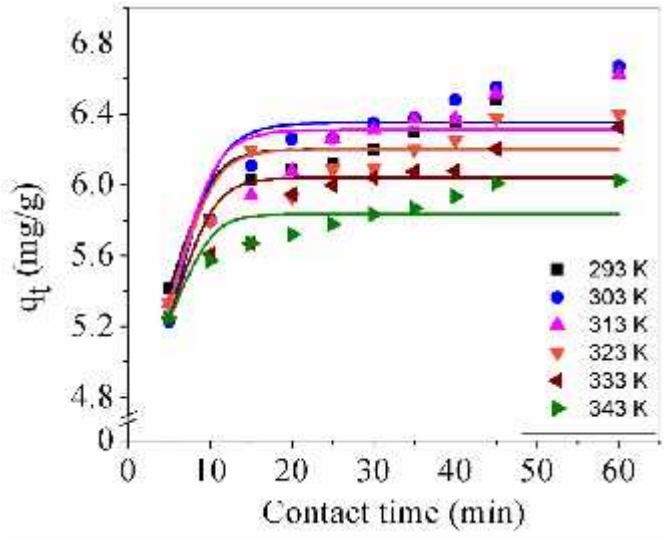

Figure 6.18 Nonlinear pseudo-first order plot of chromium removal using nano crystalline iron oxide/hydroxide obtained by error analysis function (dots represent the experimental data and lines represent the data estimated by the model)

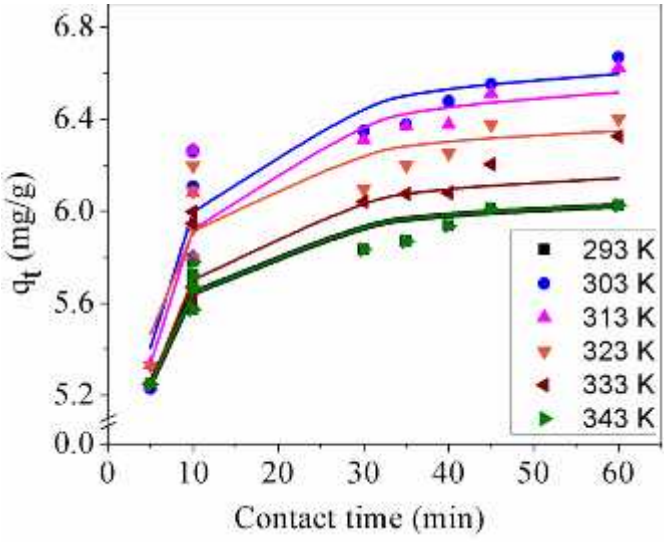

Figure 6.19 Nonlinear pseudo-second order plot of chromium removal using nano crystalline iron oxide/hydroxide obtained by error analysis function (dots represent the experimental data and lines represent the data estimated by the model)

Nonlinear analysis of kinetic data conducted via error analysis (Figures 6.18 and 6.19) and customized Microcal origin (Figures 6.20 and 6.21) methods are presented in Tables 6.10 and 6.11 respectively. In pseudo-first order model; MPSD explains the all systems better than other error functions. In pseudo-second order model; three systems out of six are better explained by MPSD and two systems by HYBRID and one system by EABS. Coefficient of determination suggested pseudo-second order model explained the system better than pseudo-first order model (Table 6.10).

Table 6.10 Pseudo-first order and pseudo-second order model constants by error analysis method for adsorption of chromium from aqueous solution on nano iron oxide/hydroxide

		Pseudo -first order				Pseudo-second order			
Temp. (K)	**Experimental q_e (mg/g)**	**Error function**	**q_e (mg/g)**	**k_1 (min^{-1})**	**R^2_{adj}**	**Error function**	**q_e (mg/g)**	**k_2 (g $mg^{-1}min^{-1}$)**	**R^2_{adj}**
293	6.56	MPSD	6.2000	0.4124	0.4792	MPSD	6.1053	0.2004	0.8577
303	6.66	MPSD	6.3485	0.3469	0.7239	HYBRID	6.7305	0.1211	0.7892
313	6.62	MPSD	6.3090	0.3733	0.5681	EABS	6.6499	0.1218	0.8204
323	6.39	MPSD	6.2000	0.3926	0.6443	HYBRID	6.4428	0.1732	0.7400
333	6.32	MPSD	6.0402	0.4062	0.5052	MPSD	6.2391	0.1696	0.7223
343	6.02	MPSD	5.8335	0.4597	0.5759	MPSD	6.1052	0.2003	0.8577

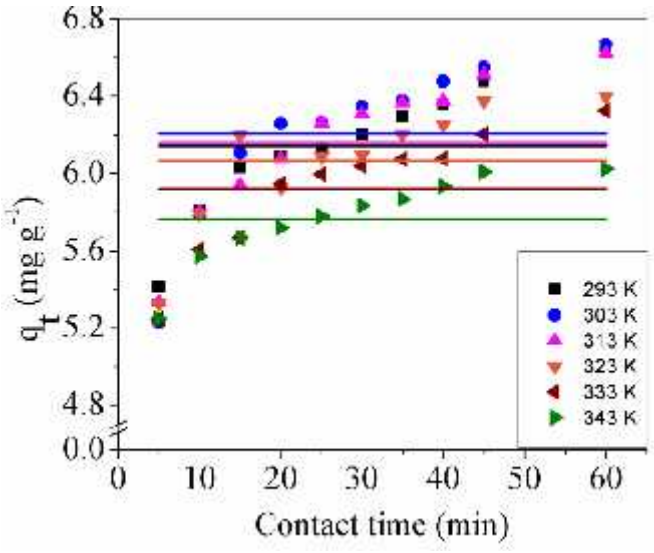

Figure 6.20 Nonlinear pseudo-first order plot of chromium removal using nano crystalline iron oxide/hydroxide obtained by customized Microcal origin function (dots represent the experimental data and lines represent the data estimated by the model)

The nonlinear pseudo-first order plot (Figure 6.20) and pseudo-second order plot (Figure 6.21) depicts the vast difference between the experimental data and data predicted by customized Microcal origin function.

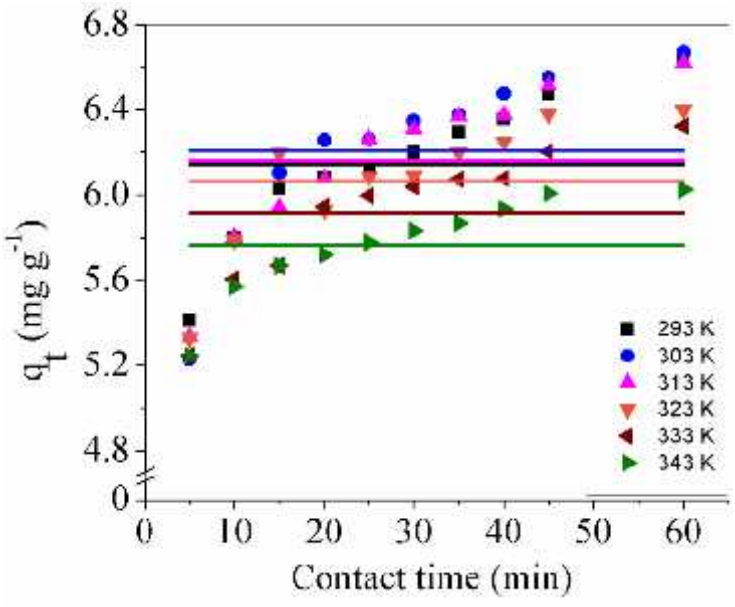

Figure 6.21 Nonlinear pseudo-second order plot of chromium removal using nano crystalline iron oxide/hydroxide obtained by customized Microcal origin function (dots represent the experimental data and lines represent the data estimated by the model)

Table 6.11 Pseudo-first order and pseudo-second order kinetic parameters for linear analysis and nonlinear analysis by Microcal origin for adsorption of chromium from aqueous solution on nano crystalline iron oxide/hydroxide

			Pseudo-first order			Pseudo-second order		
Analysis	**Temp. (K)**	**Experimental q_e (mg/g)**	**q_e (mg/g)**	**k_1 (min^{-1})**	**R^2_{adj}**	**q_e (mg/g)**	**k_2 (g $mg^{-1}min^{-1}$)**	**R^2_{adj}**
Microcal origin	293	6.56	6.1431	30.16	-0.125	6.143	3.52E+44	-0.125
	303	6.66	6.2074	26.83	-0.125	6.208	-9.37E+44	-0.125
	313	6.62	6.1606	28.82	-0.125	6.161	2.53E+44	-0.125
	323	6.39	6.0649	29.5	-0.125	6.065	-1.10E+45	-0.125
	333	6.32	5.9189	29.33	-0.125	5.919	2.01E+44	-0.125
	343	6.02	5.7655	30.52	-0.125	5.765	-3.82E+44	-0.125

Parameter determination by Microcal origin was not able to predict the kinetic parameters as its coefficient of determination is low (Table 6.11). Linear and error analysis recommended pseudo-second order model. Hence, system follows

pseudo-second order model and linear analysis is preferred due to high coefficient of determination for the present system.

6.6. Intraparticle diffusion model

Kinetic data were also fitted in intraparticle diffusion model suggested by Weber and Morris (Weber and Morris 1963). Intraparticle diffusion graph plotted between q_t and $t^{1/2}$ is shown in Figure 6.22.The k_{diff}, C_b and R^2_{adj} are shown in Table 6.12. The larger the value of intercept (C_b), bigger is the boundary layer.

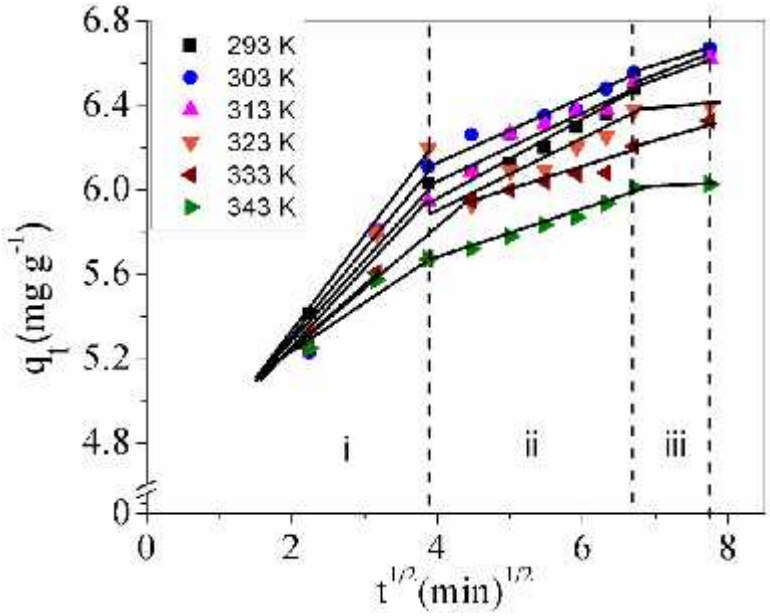

Figure 6.22 Intraparticle diffusion plot for adsorption of chromium using nano iron oxide/hydroxide

Table 6.12 Intra particle diffusion model parameters for removal of chromium using nano crystalline iron oxide/hydroxide

Temperature (K)	k_{diff} (mg/g min$^{1/2}$)	C_b (mg g^{-1})	R^2_{adj}
293	0.2033	5.1075	0.9493
303	0.2320	5.0257	0.85392
313	0.2192	5.0444	0.92589
323	0.1667	5.2159	0.75548
333	0.1828	4.9877	0.91918
343	0.1318	5.0940	0.9093

There were three regions in intraparticle diffusion plot. It depicts time dependent adsorption process. Initially, the rate of chromium uptake was faster and afterwards it slowed down with time. The region marked as ‘i’ and ‘ii’ symbolize

as dominance of film diffusion and intraparticle diffusion respectively. The region marked as 'iii' represents the region where adsorption occurs on interior surface. The intraparticle diffusion plot is not linear and does not pass through the origin. The slopes of first second and third level show deviation from origin. The deviation of slope from origin is attributed to the difference in the mass transfer rate of initial and final stages of adsorption. It validates the existence of boundary layer diffusion as rate limiting mechanism for adsorption (Mohanty *et al.* 2005).

To further investigate the actual slow step of adsorption process; kinetic data is further analyzed with Boyd model simplified by Reichenberg (Boyd *et al.* 1947;Reichenberg 1953). Boyd model differentiates adsorption rate controlling step between boundary layer and particle diffusion (diffusion inside the pores).

When the Boyd plot passes through origin; particle diffusion is dominant mechanism administrating the adsorption process. In the present case, graph (Figure 6.23) did not pass from the origin which means that the process of removal is not controlled by adsorption only, it administrated by boundary layer diffusion mechanism also.

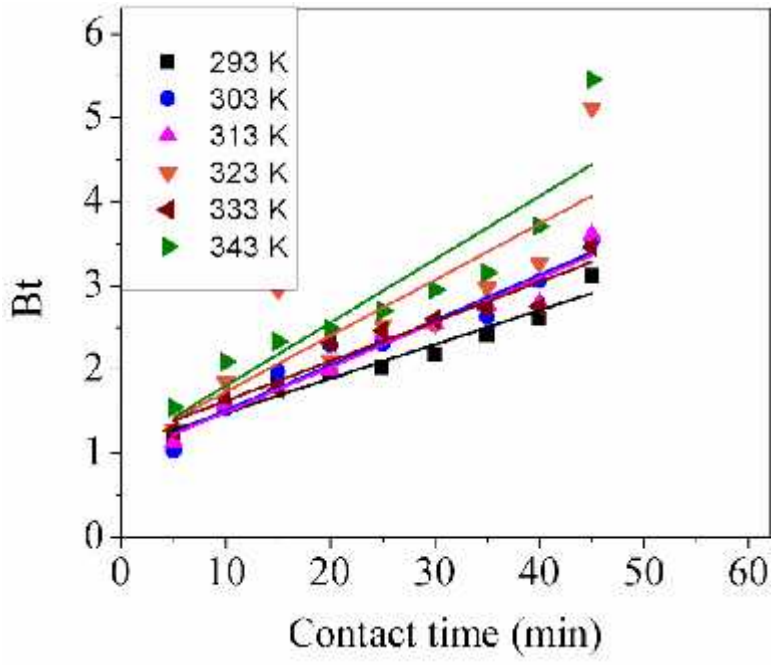

Figure 6.23 Boyd plot of for adsorption of chromium using nanocrystalline iron oxide/hydroxide

6.7. Adsorption thermodynamics

6.7.1. Determination of thermodynamic parameters using Langmuir constant method

Thermodynamic parameters i.e. change in standard free energy (ΔG^o), change in standard enthalpy (ΔH^o) and change in standard entropy (ΔS^o) were calculated using following equations (Gupta and Rastogi 2009;Liu 2009;Salvestrini *et al.* 2014):

$$\Delta G^o = -RT \ln K_L \quad (6.3)$$

$$\ln K_L = \frac{\Delta S^o}{R} - \frac{\Delta H^o}{RT} \quad (6.4)$$

Table 6.13 Thermodynamic parameters estimated by Langmuir constant method for adsorption of chromium by nano crystalline iron oxide/hydroxide (b value by Microcal origin is outrageously high hence the values are not included)

Parameter	Equation	Temp. (K)	Parameters using linear equation parameter b	Parameters using nonlinear equation parameter b
ΔG^o(kJ mol^{-1})	$\Delta G^o = -RT \ln K_L$	293	-23.75	-24.00
		303	-25.15	-30.91
		313	-25.87	-30.94
		323	-27.32	-30.77
		333	-26.84	-30.61
		343	-26.55	-26.18
ΔH^o(kJ mol^{-1})	$\ln K_L = \frac{\Delta S^o}{R} - \frac{\Delta H^o}{RT}$		9.65	-59.79*
ΔS^o(kJ mol^{-1} K^{-1})			0.1142	-0.0926*
R^2_{adj}			0.7460	0.7701*

*Parameters calculated by excluding $\ln K_L$ at 293K

The K_L is estimated from the following equation:

$$K_L = \frac{b}{\gamma} \quad (6.5)$$

$$\log \gamma = -A \quad (6.6)$$

Here, K_L (L mol^{-1}) is thermodynamic equilibrium constant was calculated from the Langmuir constant b (Liu 2009), R is universal gas constant (8.314 J $mol^{-1}K^{-1}$), T is the temperature, γ_e is the activity coefficient, I_e is the ionic strength (1.1 x 10^{-3} mol/kg) of the solute at equilibrium, A_1 is a constant (0.509 $mol^{-1/2}$ $kg^{1/2}$) and z is the charge on ion. The ΔH^o and ΔS^o were calculated from the slope and intercept of plot between $\ln K_L$ and 1/T respectively (Elkady *et al.* 2011). The calculated values ΔG^o, ΔH^o and ΔS^o parameters are presented in the Table 6.13.

Comparison of thermodynamic parameter by linear and non-linear curve fitting derived Langmuir constant i.e. b showed variation in magnitude and sign afore to magnitude. Both the methods suggested that current adsorption process was spontaneous. However, nonlinear method suggested the system is exothermic and occurs with decrease in entropy. Whereas, linear method endorsed that the system is endothermic and takes place with increase in entropy. But the R^2_{adj} of fitted curve ($\ln K_L$ *vs.* 1/T) is better for linear method than nonlinear method. Hence, this method is used to determine isotherm parameters.

The positive value of enthalpy change via linear method (ΔH^o = 9.65 kJ mol^{-1}) attributed towards the endothermic nature of the adsorption process. Negative values of ΔG^o indicated that the process is spontaneous in nature. The ΔG^o becomes more negative with rise in temperature indicating that the process becomes more feasible at higher temperatures. The positive values of ΔS^o (0.1142 kJ mol^{-1}) indicate the increase of disorderness at adsorbate-adsorbent interface during adsorption of chromium in present case.

6.7.2. Determination of thermodynamic parameters using partition method

In addition to Langmuir constant method, partition method is also used to determine the thermodynamic parameters. Here K_p of K_C is used in place of K_L and K_p is determined as follows (Salvestrini *et al.* 2014):

$$K_c \text{ or } K_p = \frac{C_s}{C_w} \quad (6.7)$$

Where, C_s and C_w depict the concentration of adsorbate in solid and liquid phase. After determination of K_p, Equations 6.3 and 6.4 were used for determination of

thermodynamic parameters. In addition to this, free energy change is also calculated from following equation (Salvestrini *et al.* 2014):

$$\Delta G_{\circ} = \Delta H_{\circ} - T\,\Delta S_{\circ} \qquad (6.8)$$

The negative values of enthalpy change (ΔH^{o} = -71.06 kJ mol^{-1}) in Table 6.14 depicts the exothermic nature of the adsorption process. Spontaneous nature of the adsorption system is depicted by negative values of ΔG^{o} .The value of ΔG^{o} becomes less negative with increase of temperature pointing towards lower feasibility of process at higher temperatures. The negative value of ΔS^{o} (-0.1708 kJ mol^{-1}) indicates the decrease of disorderness at adsorbate-adsorbent interface during adsorption of chromium. The value of change in free energy calculated from equation 6.8 is alike the change in free energy calculated from equation 6.5. The free energy, enthalpy and entropy change calculated from both methods show negative sign before the values, which prove the system to be spontaneous, exothermic and occurs with increase in randomness of system. There is difference in the change in free energy values calculated with the help of Langmuir constant (Liu 2009).

Table 6.14 Thermodynamic parameters calculated by partitioned method for adsorption of chromium by nano crystalline iron oxide/hydroxide

Temp. (K)	**ΔG^{o} (kJ mol^{-1})**	**ΔH^{o} (kJ mol^{-1})**	**ΔS^{o} (kJ mol^{-1} K^{-1})**	**R^2adj**	**ΔG^{o} (kJ mol^{-1})**
	$\Delta G^{o} = -RT\ln K^{p}$	$\ln K^{p} = \frac{\Delta S^{0}}{R} - \frac{\Delta H^{0}}{RT}$			$\Delta G^{o} = \Delta H^{o} - T\Delta S$
293	-19.23	-71.065	-0.1708	0.8532	-21.00
303	-20.20				-19.29
313	-19.61				-17.58
323	-15.60				-15.87
333	-14.90				-14.16
343	-10.81				-12.46

Aforementioned methods suggested that the system is spontaneous, but with variation in magnitude. As K_c or K_p is equal to thermodynamic equilibrium

constant (K_L) only at dilute concentration (Liu 2009), thermodynamic parameters estimated by Langmuir constant method are preferred over partition method.

6.7.3. Activation Energy

Arrhenius equation is used to determine activation energy for adsorption (Arrhenius 1889). The Arrhenius equation is depicted by subsequent equation (Chen *et al.* 2013):

$$\ln k_2 = \ln A - E_a/ RT \quad (6.9)$$

Where k_2 (g mg $^{-1}$ min^{-1}) represents the rate constant obtained for the pseudo-second order kinetic model, E_a (J mol^{-1}) is the Arrhenius activation energy of adsorption and A is the Arrhenius factor. The slope of $-E_a/R$ is obtained by a plot between $\ln k_2$ against 1/T. The activation energy calculated is 9.39 kJ mol^{-1}.

6.8. Desorption experiments

Three desorbing agents namely sodium hydroxide, ammonium hydroxide and potassium hydroxide (0.1 N for each solutions) solutions were used for regeneration of the adsorbent (Table 6.15).

Table 6.15 Desorption efficiency of 0.1N NaOH, 0.1N KOH, 0.1N NH_4OH for chromium loaded nano crystalline iron oxide/hydroxide

S.No.	Desorbing agent	Desorption efficiency
1	0.1 N NaOH	90.97
2	0.1N KOH	88.81
3	0.1N NH_4OH	72.36

Among all bases, sodium hydroxide showed the best results in regenerating the iron oxide/hydroxide for reuse for removal of chromium. Sodium hydroxide regenerates the adsorbent up to five cycles with excellent results (Table 6.16).Thus, on the basis of results, NaOH is recommended for regeneration of the nanocrystalline iron oxide/hydroxide, especially for the removal of chromium from its aqueous solutions.

Table 6.16 Chromium removal after subsequent regeneration cycle (Initial concentration = 50 mg L^{-1}, pH = 2, Adsorbent dose = 4 g L^{-1}, Temperature =303 K)

S.No.	Regeneration cycle	Chromium removal (%) after regeneration cycle
1	1^{st}	99.01
2	2^{nd}	98.68
3	3^{rd}	98.68
4	4^{th}	94.73
5	5^{th}	97.36

6.9. Conclusions

Chromium was effectively removed from aqueous solutions using nanocrystalline iron oxide/hydroxide as an adsorbent. The adsorption equilibrium time was 60 min. The pH was most dominating factor for removal of chromium using nano crystalline iron oxide/hydroxide. The most dominant factor pH was followed by factors i.e. adsorbent and initial concentration affecting adsorption of chromium. However, temperature did not significantly affect the removal of chromium from aqueous solutions. Optimum parameters were initial concentration, pH, adsorbent dose and temperature at 20 mg L^{-1}, 2 to 2.5 and 11 g $L^{-1}$and 303 K respectively. The isotherm and kinetic models data fitted better with linear curve fitting analysis. The data for chromium removal by nanocrystalline iron oxide/hydroxide follows Langmuir isotherm model and pseudo-second order kinetic model. The change in Gibbs free energy was negative showing spontaneous nature of the adsorption process. The adsorption of chromium using nanocrystalline iron oxide/hydroxide was endothermic in nature and occurred with increase of entropy. The regeneration of the adsorbent was done with sodium hydroxide and showed steady results up to five regeneration cycles.